Creep failure of reformer tubes in a petrochemical plant

Bahrami, Abbas; Taheri, Peyman

DOI
10.3390/met9101026

Publication date
2019

Document Version
Final published version

Published in
Metals

metals

MDPI

Article

Creep Failure of Reformer Tubes in a Petrochemical Plant

Abbas Bahrami [1] and Peyman Taheri [2,*]

[1] Department of Materials Engineering, Isfahan University of Technology, Isfahan 84156-83111, Iran; a.n.bahrami@cc.iut.ac.ir

[2] Delft University of Technology, Department of Materials Science and Engineering, Mekelweg 2, 2628 CD Delft, The Netherlands

* Correspondence: p.taheri@tudelft.nl; Tel.: +31-15-278-2275

Received: 27 August 2019; Accepted: 20 September 2019; Published: 21 September 2019

Abstract: This paper investigates a failure in HP-Mod radiant tubes in a petrochemical plant. Tubes fail after 90,000 h of working at 950 °C. Observed failure is in the form of excessive bulging and longitudinal cracking in reformer tubes. Cracks are also largely branched. The microstructure of service-exposed tubes was evaluated using optical and scanning electron microscopes (SEM). Energy-dispersive X-ray spectroscopy (EDS) was used to analyze and characterize different phases in the microstructure. The results of this study showed that carbides are coarsened at both the inner and the outer surface due to the long exposure to a carburizing environment. Metallography examinations also revealed that there are many creep voids that are nucleated on carbide phases and scattered in between dendrites. Cracks appeared to form as a result of creep void coalescence. Failure is therefore attributed to creep due to a long exposure to a high temperature.

Keywords: reformer tubes; HP-Mod; failure analysis; creep

1. Introduction and Case Background

Hydrogen is produced in the so-called "steam reforming" process, in which a steam/hydrocarbon mixture goes through vertical reforming tubes. Hydrocarbon is then transformed to hydrogen and carbon monoxide. Creep-resistant centrifugally cast high Cr/high Ni tubes are widely used in reformer units in petrochemical plants for hydrogen production [1]. HK40 (Cr25Ni20), HP40 (Cr25Ni35), and HP-Mod (Cr25Ni35Nb) are examples of currently used heat resistant alloys with superior high temperature corrosion and creep resistance. Reformer tubes experience a severe working condition, i.e., the working temperature is as high as 1000 °C and pressures are up to 3.5 MPa [2,3]. These tubes are expected to have a service life over 100,000 h, with strains no more than 3%, at temperatures and internal pressures up to 980 °C and 35 bar, respectively [4]. Hoop stress, originated from internal pressure, together with constant high temperature service exposure results in creep stress approximately equal to 30 MPa. This in turn results in a creep deformation rate of approximately 10^{-10} s^{-1} [3]. It is therefore not surprising that reformer tubes are considered very critical components when it comes to the safe operation and the integrity of installations in a petrochemical/reforming plant. In addition, from an economic standpoint, these tubes are strategically important. Obviously, shutdowns in a petrochemical plant due to failures in reformer tubes are very costly [5]. Moreover, tube replacement operations require an extensive dismantling of the furnace components. A total replacement operation can last a few days and can easily cost millions of dollars for a petrochemical plant. With that said, one can imagine that understanding and mitigating or postponing failures in reformer tubes are very important. This paper investigates a failure in reforming tubes, made of HP-Mod alloy, after 90,000 h of service

exposure at approximately 950 °C. The results, obtained from this root cause failure analysis, can be used in assessing and mitigating similar failures in reforming units.

2. Experimental Methods

Samples for microstructure and failure analyses were taken from failed tubes. According to the specification, the alloy is HP-Mod. The chemical composition of samples was measured, using inductively-coupled plasma atomic energy spectroscopy (ICPAES). Optical and scanning electron microscopes (SEM Philips XL30, Philips, Eindhoven, The Netherlands) were used to investigate the microstructure of failed specimens. Energy-dispersive X-ray spectroscopy (EDS, Ametek, PA, USA) was used to characterize different phases in the microstructure. Fractography was performed on the fracture surface of failed specimens.

3. Results and Discussion

3.1. Visual Examinations

Figure 1 shows an example of failed reformer tubes together with an image, showing how tubes are installed in a reforming unit. As can be seen, cracks have propagated longitudinally. Extensive branching is also observed overall on the outer surface. It is also noticeable that in some parts tubes are largely deformed in such a way that a clear bulging is observed. Cracks are often seen in areas of localized deformation/bulging.

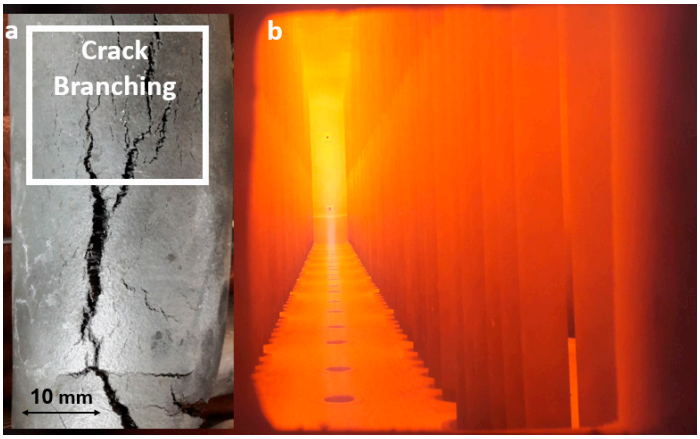

Figure 1. (**a**) Example of failed tubes and (**b**) an image of tubes in service.

3.2. Microstructure and Chemical Analyses

The chemical composition of the alloy was measured to make sure that the chemical composition of the failed tubes falls within the standard range. Table 1 shows the chemical composition of a failed specimen, showing that the alloy has a typical composition of a HP-Mod alloy.

Table 1. Chemical composition of failed specimens.

Composition	C	Si	Mn	Cr	Ni	Nb	Fe
wt%	0.41	1.2	0.9	25.5	35.6	1.3	Bal.

Optical and SEM micrographs of service-exposed tubes are shown in Figure 2. As can be seen, there are two types of morphologies for primary eutectic phases in the matrix. Primary eutectic phases can be categorized into "Chinese script" morphology (see Figure 2a) and a rather continuous grain boundary phase morphology (see Figure 2b). EDS analyses show that the eutectic phase is a mixture of dark and white phases, with the former ones being chromium carbides (Figure 2c), and more

specifically $M_{23}C_6$ and M_7C_3 carbides (M = Fe, Cr) ($M_{23}C_6$ carbides reportedly gradually transform to M_7C_3 carbides during the service due to carbon diffusion/carburization [6,7]), with the latter being niobium carbide (Figure 2d).

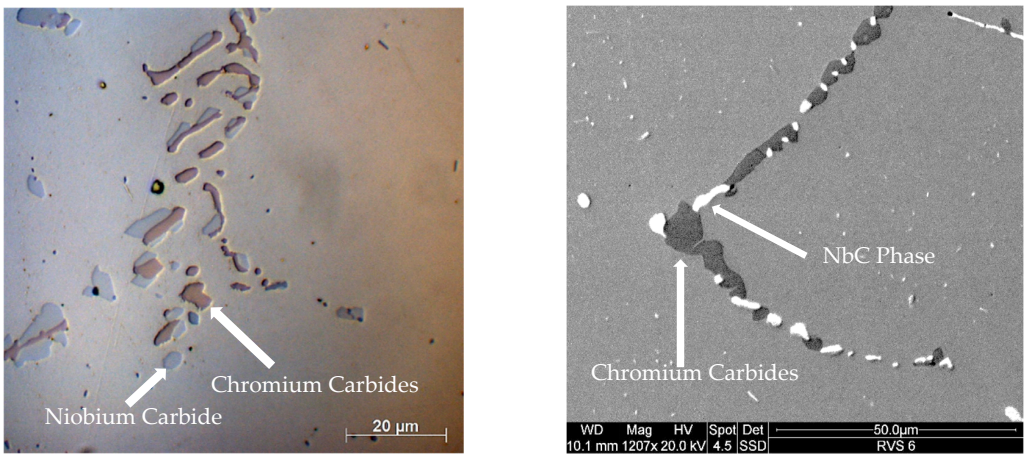

(**a**) (**b**)

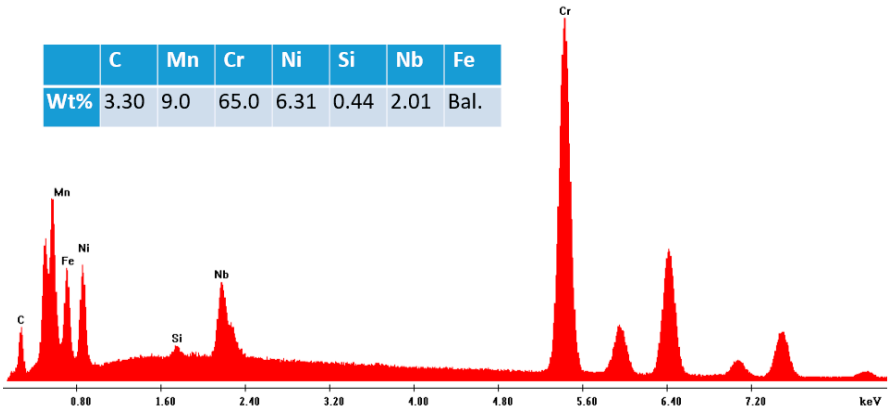

	C	Mn	Cr	Ni	Si	Nb	Fe
Wt%	3.30	9.0	65.0	6.31	0.44	2.01	Bal.

(**c**)

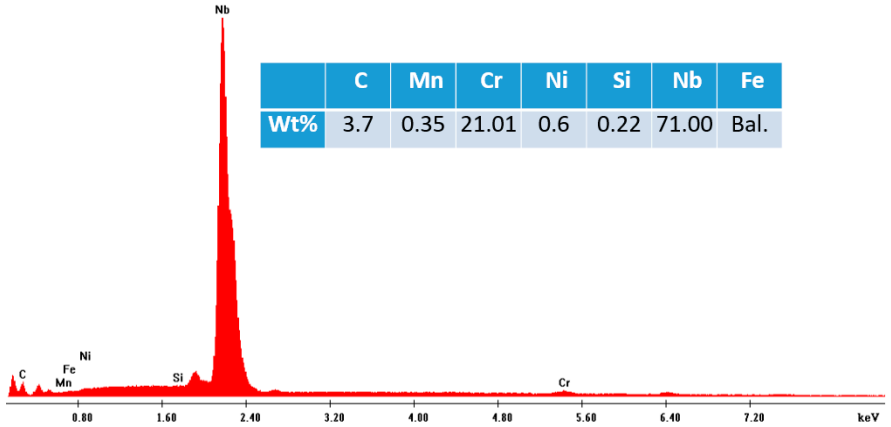

	C	Mn	Cr	Ni	Si	Nb	Fe
Wt%	3.7	0.35	21.01	0.6	0.22	71.00	Bal.

(**d**)

Figure 2. (**a**) Optical and (**b**) SEM images of the microstructure in failed tubes, together with EDS analyses of the (**c**) black phase (chromium carbide) and (**d**) white phase (NbC).

Figure 3 shows a stereomicroscope image of the cross section of the failed tube. Based on this image, the grain structure can be divided into an elongated dendritic structure from the outer surface towards the half thickness, and an equiaxed grain structure from the half thickness towards the inner surface. This is a typical grain structure in centrifugally cast tubes in which solidification starts from the outer surface, followed by dendrite growth towards the center of tube. Equiaxed grains are then formed at the latest stage of solidification. In addition, it is noticeable that the examined cross-section exhibits a large number of voids. In the dendritic area, voids have more directionality and are more oriented alongside dendrite growth direction, while those in the equiaxed grain area are randomly distributed. Figure 4a,b compares the microstructure of the degraded sample with that in the as-cast condition, clearly showing how voids are formed due to longtime service exposure. In addition, Figure 4 shows optical images of voids in both dendritic structure and equiaxed structure zones. It is seen that voids in the former zone have a clear directionality and are fully connected in some areas (see Figure 4b,c). It appears that cracks are formed as a result of void coalescence. On the contrary, voids in the equiaxed structure are more randomly distributed, are more isolated and are less connected (see Figure 4c,d). It is postulated that in the case that creep prevails, embrittlement can take place, resulting in a decreased rupture ductility [8,9]. Creep and rupture strengths are considered to be extremely important design parameters [10]. Deterioration of rupture ductility due to creep largely influences crack growth rates and high temperature damage tolerance of reformer tubes. It has been hypothesized [11] that the mechanism of creep-induced embrittlement is linked to the generation and coalescence of intergranular voids, which are controlled by the formation of a denuded zone in the vicinity of the precipitates. The denuded zone around the precipitates is formed due to the segregation and diffusion of alloying elements at the precipitate/matrix interfaces. Our results show that, in this case, a network of voids has nucleated and grown during creep deformation. It appears that the failure mechanism in this case is due to the nucleation of creep voids and their evolution into microcracks, and finally macrocracks. Buchheim et al. [12] postulated that creep cracking due to long-term high temperature service can take place in the piping components and can grow due to temperature fluctuations, particularly during abrupt shutdowns. Pourmohammad et al. [5] also discussed the negative implications of sudden shutdowns for the lifetime of radiant tubes. When it comes to the creep failure of reformer tubes, the first stage is always related to the void nucleation [13–16]. Figure 5 shows that creep voids have nucleated on both chromium carbide and niobium carbide particles. Given that $M_{23}C_6$ and NbC carbides are distributed in the inter-dendritic regions [2], voids are also nucleated and distributed in-between dendrites. Figure 6 shows that, in some areas, voids are formed in between carbide particles. The working temperature of reformer tubes is high enough to cause carbide coalescence and coarsening. Fine carbide precipitates obviously enhance the creep resistance of HP-Mod alloys. Yet, in the coalesced and coarsened carbide structure, the positive attribution of carbide particles to the creep resistance of HP-Mod alloys can reverse. Coarse carbide particles can act as creep void nucleation sites. Carbide coalescence and coarsening reactions are diffusion-dependent, inferring that a slight increase in service temperature can significantly accelerate both carbide coalescence and coarsening, and this in turn results in faster nucleation of creep voids. This clearly adversely affects the creep lifetime of HP-Mod alloys. In comparison to chromium carbides, niobium carbides have a comparatively higher melting point, giving them more stability during high temperature service conditions. Rampat et al. [2] postulated that "since most of the NbC precipitates are out of the matrix and remain on the grain and/or cell boundaries, higher activation energies (via higher stresses and temperatures) are required for slip and the consequential creep voids". The results of this study depict that both chromium and niobium carbides are nucleation sites for creep voids. Examples from both cases are shown in Figure 5. Creep-induced embrittlement and distribution of voids in the microstructure lead to an easier crack propagation and transition of fracture modes. This is evidently seen in Figure 7. As can be seen in this figure, the fracture surface close to the outer surface in the dendritic region has a directional fibrous appearance. Voids are also clearly seen on the fracture surface. There is no indication of dimples anywhere on the fracture surface, supporting the

argument of creep-induced embrittlement in failed tubes [17]. However, the pictures do not show ordinary intergranular or interdendritic fractures. It is likely that the fracture surface was altered by the interaction with the steam/hydrocarbon/hydrogen atmosphere.

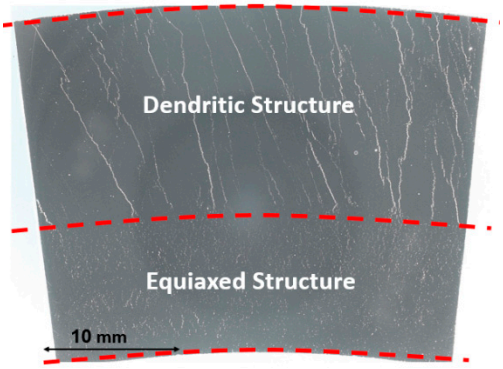

Figure 3. Stereomicroscope image of the cross section of the failed tube.

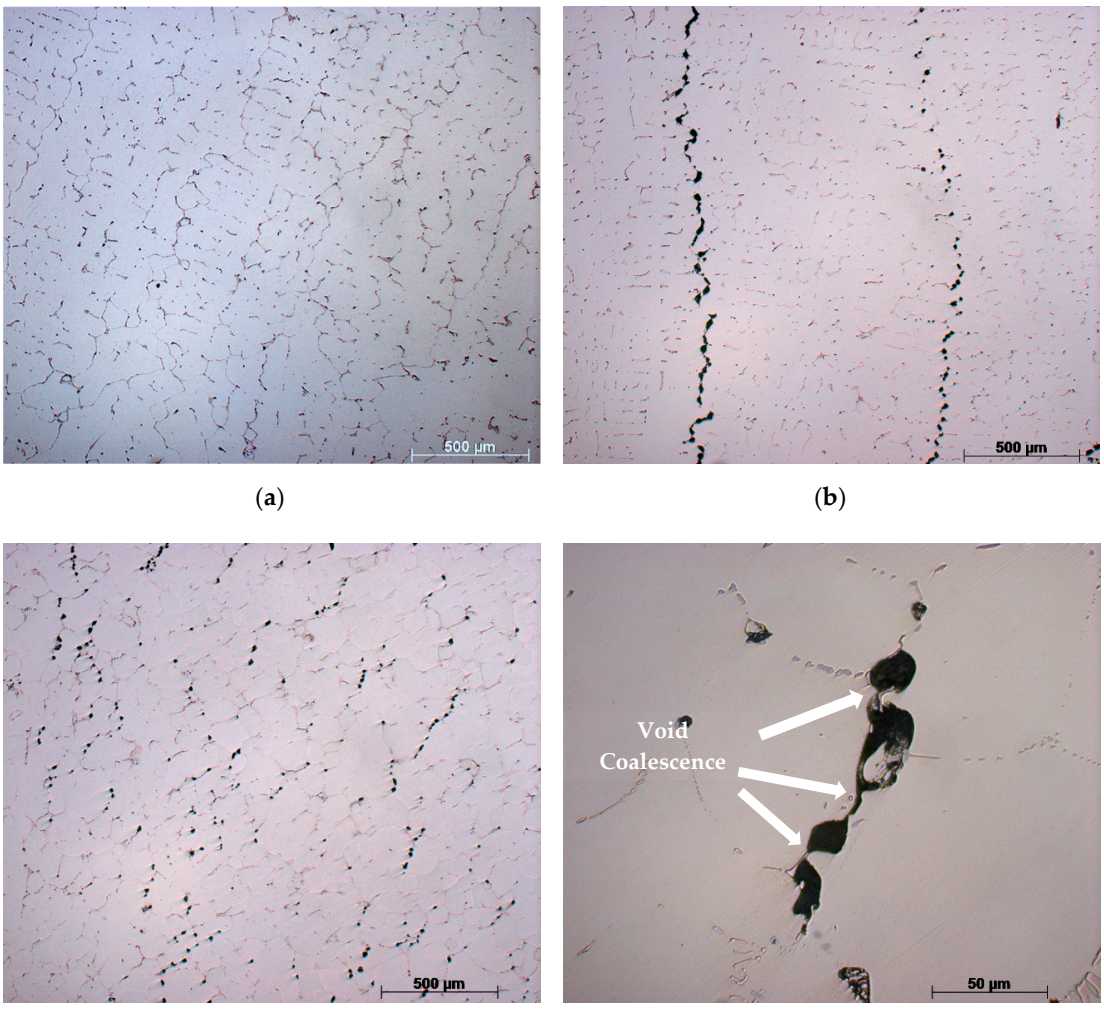

(**a**) (**b**)

(**c**) (**d**)

Figure 4. (**a**) The as-cast microstructure and voids in failed samples in (**b**) the dendritic structure region and (**c**,**d**) the equiaxed grain region.

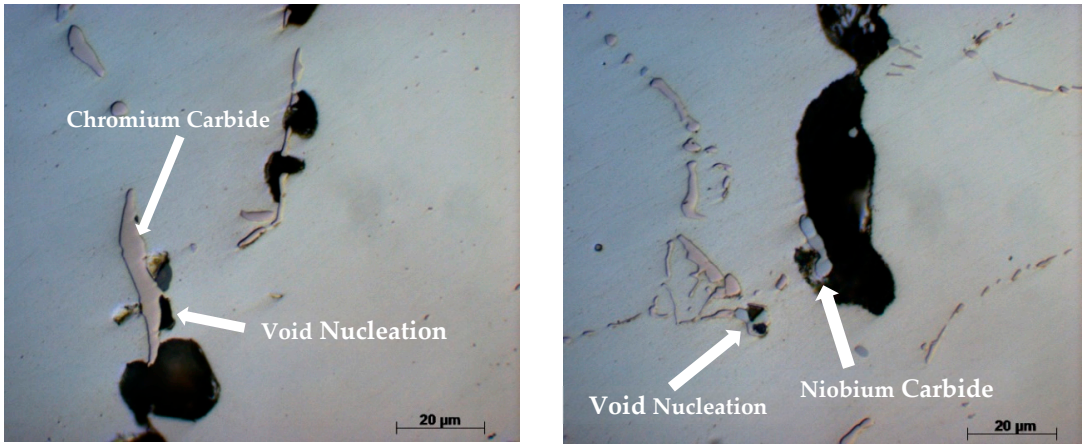

(**a**) (**b**)

Figure 5. Void nucleation on (**a**) chromium carbide and (**b**) niobium carbide particles.

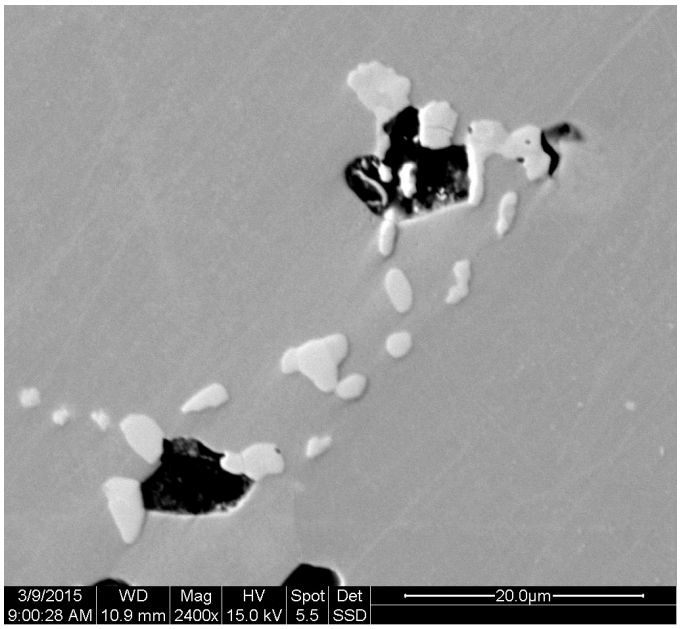

Figure 6. Creep voids are often nucleated in-between particles.

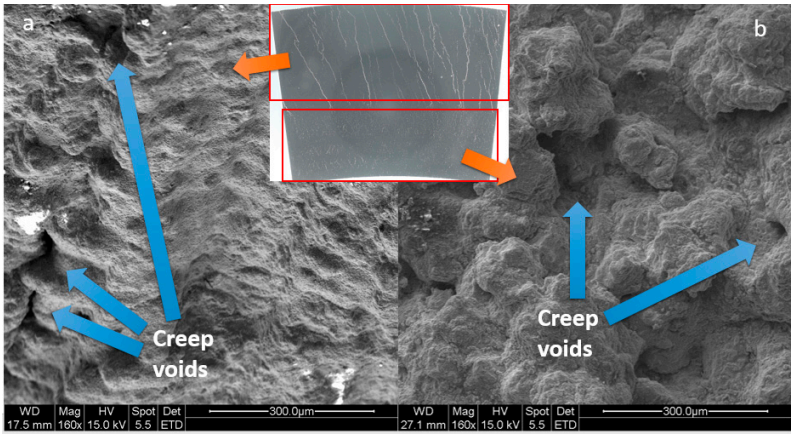

Figure 7. Fracture surface in (**a**) dendritic and (**b**) equiaxed grain regions.

4. Concluding Remarks

This paper investigated the root cause analysis of failure in HP-Mod radiant tubes in a petrochemical plant. Failure was reported after 90,000 h of working at 950 °C. Longitudinal cracks with lots of branching were observed on failed tubes in such a way that these tubes could not be used again due to crack and excessive creep deformation. The results of failure analysis showed that:

- Tubes have two typical grain structures: (i) dendritic microstructure, starting from the outer surface towards the half-thickness, and (ii) equiaxed grain structure, starting from the half thickness towards the inner surface. This is the typical microstructure of centrifugally cast heat resistant alloys.
- Two types of carbides were present in the microstructure: (i) chromium-rich carbides and (ii) niobium carbides. In most cases, carbides had a "Chinese script" morphology. Carbides were overall coalesced and coarsened to a large extent.
- Creep voids were observed through the thickness of failed tubes. Voids in the dendritic structure region were oriented more alongside dendrites and were seen more often in the inter-dendritic regions. On the contrary, voids in the equiaxed grain structure were more randomly distributed without any directionality.
- Creep voids were nucleated on both chromium and niobium carbides. Cracks were formed due to the growth and coalescence of voids.
- The root cause analysis of the concerned failure showed that tubes failed due to creep failure.
- When it comes to creep failure, the most important factor that controls the lifetime of the components during a high temperature service is temperature. Improper control of temperature and overheating can dramatically decrease the creep lifetime of reformer tubes.

Author Contributions: Conceptualization, A.B.; methodology, A.B.; formal analysis, A.B.; investigation, A.B. and P.T.; writing—original draft preparation, A.B.; writing—review and editing, P.T.; visualization, A.B.; supervision, P.T.; project administration, P.T.

Funding: This research received no external funding.

Acknowledgments: Authors would like to thank Delft University of Technology for support in publishing this manuscript.

Conflicts of Interest: The authors declare no conflict of interest.

References

1. Jones, D.R.H. Creep failures of overheated boiler, superheater and reformer tubes. *Eng. Fail. Anal.* **2004**, *11*, 873–893. [CrossRef]
2. Rampat, K.; Maharaj, C. Creep embrittlement in aged HP-Mod alloy reformer tubes. *Eng. Fail. Anal.* **2019**, *100*, 147–165. [CrossRef]
3. Guglielmino, E.; Pino, R.; Servetto, C.; Sili, A. Creep damage of high alloyed reformer tubes. In *Handbook of Materials Failure Analysis with Case Studies from the Chemicals, Concrete and Power Industries*; Butterworth-Heinemann: Oxford, UK, 2016; pp. 69–91.
4. Swaminathan, J.; Guguloth, K.; Gunjan, M.; Roy, P.; Ghosh, R. Failure analysis and remaining life assessment of service exposed primary reformer heater tubes. *Eng. Fail. Anal.* **2008**, *15*, 311–331. [CrossRef]
5. Pourmohammad, H.; Bahrami, A.; Eslami, A.; Taghipour, M. Failure investigation on a radiant tube in an ethylene cracking unit. *Eng. Fail. Anal.* **2019**, *104*, 216–226. [CrossRef]
6. Tari, V.; Najafizadeh, A.; Aghaei, M.H.; Mazloumi, M.A. Failure analysis of ethylene cracking tube. *J. Fail. Anal. Prev.* **2009**, *9*, 16–32. [CrossRef]
7. Otegui, J.L.; De Bona, J.; Fazzini, P.G. Effect of coking in massive failure of tubes in an ethylene cracking furnace. *J. Eng. Fail. Anal.* **2015**, *48*, 201–209. [CrossRef]
8. American Petroleum Institute. *API 942B Material, Fabrication, and Repair Considerations for Austenitic Alloys Subject to Embrittlement and Cracking in High Temperature 565 °C to 760 °C Refinery Services*; API: Washington DC, USA, 2017.

9. Barcik, J. Mechanism of σ-phase precipitation in Cr–Ni austenitic steels. *Mater. Sci. Technol.* **1988**, *4*, 5–15. [CrossRef]
10. Zieliński, A.; Dobrzański, J.; Purzyńska, H.; Golański, G. Properties, structure and creep resistance of austenitic steel Super 304H. *Mater. Test.* **2015**, *57*, 859–865. [CrossRef]
11. Villanueva, D.M.E.; Junior, F.C.P.; Plaut, R.L.; Padilha, A.F. Comparative study on sigma phase precipitation of three types of stainless steels: austenitic, superferritic and duplex. *Mater. Sci. Technol.* **2006**, *22*, 1098–1104. [CrossRef]
12. Buchheim, G.; Becht, C.; Nikbin, K.; Dimopolos, V.; Webster, G.; Smith, D. Influence of aging on high-temperature creep crack growth in type 304H stainless steel. In *Nonlinear Fracture Mechanics: Volume I Time-Dependent Fracture*; ASTM International: West Conshohocken, PA, USA, 1988.
13. Song, R.; Wu, S. Microstructure evolution and residual life assessment of service exposed Cr35Ni45 radiant tube alloy. *J. Eng. Fail. Anal.* **2018**, *88*, 63–72. [CrossRef]
14. Khodamorad, S.H.; Haghshenas Fatmehsari, D.; Rezaiea, H.; Sadeghipour, A. Analysis of ethylene cracking furnace tubes. *J. Eng. Fail. Anal.* **2012**, *21*, 1–8. [CrossRef]
15. Alvino, A.; Lega, D.; Giacobbe, F.; Mazzocchi, V.; Rinaldi, A. Damage characterization in two reformer heater tubes after nearly 10 years of service at different operative and maintenance conditions. *J. Eng. Fail. Anal.* **2010**, *17*, 1526–1541. [CrossRef]
16. Guan, K.; Xu, H.; Wang, Z. Analysis of failed ethylene cracking tubes. *J. Eng. Fail. Anal.* **2005**, *12*, 420–431. [CrossRef]
17. Monobe, L.S.; Shiguenobu, L.; Schön, C.G. Microstructural and fractographic investigation of a centrifugally cast 20Cr32Ni+Nb alloy tube in the 'as cast' and aged states. *J. Mater. Res. Technol.* **2013**, *2*, 195–201. [CrossRef]